Chapter- 6

Results and Discussion

Erosive wear properties of CNTs, GO, and (CNTs/GO) hybrid coated carbon FREC using Taguchi orthogonal array

This chapter investigates the erosion wear performance of polymer composites reinforced with CNTs, GO, and hybrid (GO/CNTs) coated carbon fibers, emphasizing fiber surface modification for enhanced fiber-matrix adhesion and load transfer. Solid particle erosion tests assess the influence of velocity, discharge rate, and impingement angle on wear resistance. The Taguchi method, employing an orthogonal array approach, optimizes experimental efficiency by analyzing multiple variables without exhaustive testing. ANOVA quantifies factor significance and interactions, ensuring statistical robustness. These techniques systematically enhance product and process quality by identifying key experimental variables. SEM analysis of worn surfaces characterizes dominant erosion wear mechanisms providing insights into factors influencing wear resistance.

6.1 Erosion test

Erosive wear occurs when solid particles suspended in a fluid stream, whether liquid or gas, collide with the surfaces of elements, causing material loss over time. In this present work particularly the testing process, arid compressed air is mixed with particles consistently using an alumina powder flow regulator before being propelled through a converging brass nozzle with an internal diameter of 1.5mm. Erosive wear is caused when these air jet alumina particles collide with solid surfaces. This arrangement establishes uniform erosive conditions essential for assessing the erosion resistance of produced epoxy-composite samples. Aluminum oxide (Al_2O_3) served as the erodent in this study,

with particles observed to exhibit both angular and round shapes, as evidenced by the SEM micrograph showed in Figure 6.1 (a).

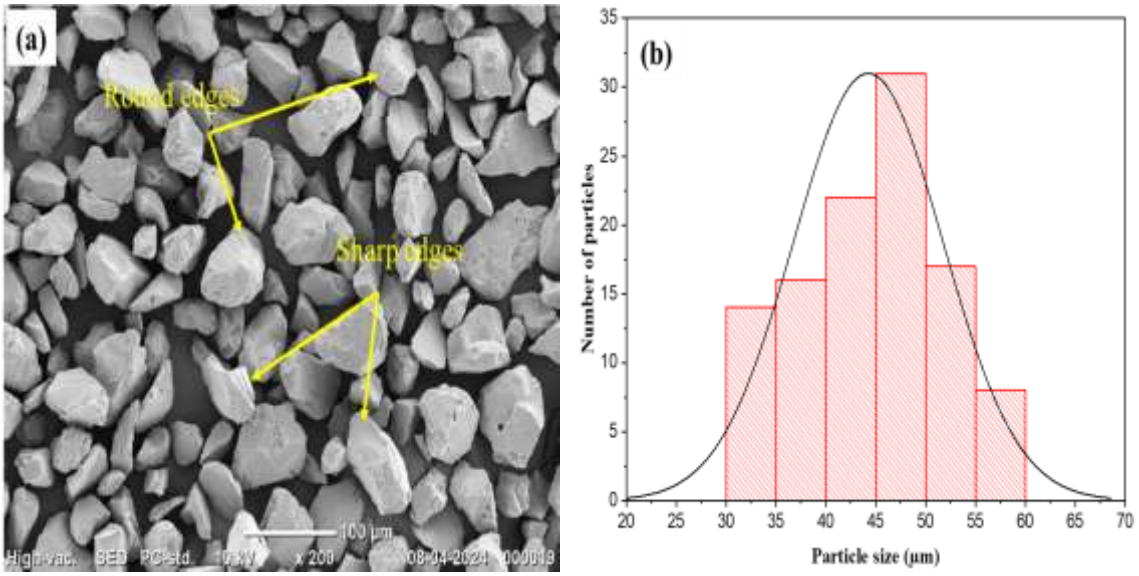

Figure 6.1 Representative (a) SEM images of Aluminum oxide erodent particles, (b) Particle size distribution of erodent (Al_2O_3).

The average size of the eroded particles was determined to be 45 µm, and their distribution is illustrated in Figure 6.1(b). The composite notation and specifications of different composite materials are shown in Table 6.1. Erosion rates of each composite specimen were computed using Equation (6.1), considering various process parameters such as coating materials, impact velocity, discharge rate, impingement angle, and operational levels, as detailed in Table 6.2. The different composite samples used for erosion tests are shown in Figure 6.2(a). Procedural steps for conducting erosion tests on fiber-based polymer composites are illustrated in Figure 6.2(b). Each sample underwent cleaning with acetone, drying, and precise weighing to an accuracy of ±0.1 mg using a precision electronic balance.

$$\text{Erosion rate} = \left(\frac{\text{Weight of specimen before test} - \text{Weight of specimen after test}}{\text{Erodent discharge rate x Exposer time}}\right)\left(\frac{g}{g}\right) \quad (6.1) \quad [249]$$

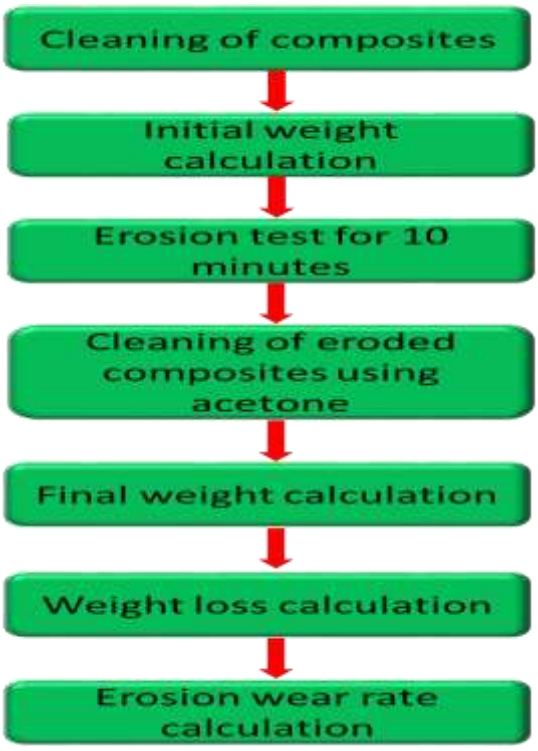

(a) **(b)**

Figure 6.2 Representatives (a) Erosion test composite samples, and (b) Steps were carried out for the erosion investigate of polymer composites.

Table 6.1 Comprehensive details regarding composite notations and specifications

Composite notations	Composite specification
C_1	Uncoated Carbon fiber reinforced epoxy composite (CFRE)
C_2	GO coated Carbon fiber reinforced epoxy composite (GCFRE)
C_3	CNTs coated Carbon fiber reinforced epoxy composite (CCFRE)
C_4	Hybrid (CNTs/GO) coated Carbon fiber reinforced epoxy composite (HCFRE)

Table 6.2 Controlling factors and levels of the variables used in Air jet erosion tester

	Levels				
Control Factor	I	II	III	IV	Units
Coating material	Uncoated (U)	GO (G)	CNTs (C)	Hybrid (H)	unit less
Discharge rate	2	3	4	5	g/min
Impact velocity	20	40	60	90	m/s
Impingement angle	15	30	60	90	degree

6.2 Experimented results of erosion wear test and Taguchi analysis

A comprehensive investigation was conducted to optimize parameters for carbon fiber and nanoparticle-coated carbon fiber epoxy composite materials. The experimental results about erosion wear on the carbon-epoxy composites (designated as C_1, C_2, C_3, and C_4) were presented. Additionally, the Taguchi (L_{16}) orthogonal array was utilized to streamline the number of test runs, as shown in Table 6.3, specifically designed for polymer-based composites. The combination of parameters that resulted in the lowest erosion rate seen in the epoxy composites was explained by the analysis of the data [250]. Figure 6.3 and 6.4 illustrate the influence of control parameters on the erosion wear rate. In Figure 6.3, the main effects plots of S/N ratios are depicted, while Figure 6.4 showcases the main effects plot for data means. The response table and the signal-to-noise ratio for means obtained from the Taguchi analysis are presented in Tables 6.4 and 6.5, respectively. Table 6.4 identifies the principal factor influencing the S/N ratio of erosion wear rate, whereas Table 6.5 identifies the principal factor influencing the mean of means for erosion wear rate.

Table 6.3 Taguchi (L_{16}) parameters and Erosion rate results of epoxy composite samples.

Test run	Coating material	Impact velocity m/s	Discharge g/min	Impingement angle Degree	Erosion rate ($x10^{-5}$ g/g)	S/N Ratio (dB)
1	U	20	2	15	6.2457	-15.9116
2	U	40	3	30	9.1234	-19.2031
3	U	60	4	60	14.5478	-23.2559
4	U	90	5	90	19.3547	-25.7357
5	G	20	3	60	5.7456	-15.1867
6	G	40	2	90	10.8475	-20.7065
7	G	60	5	15	9.2354	-19.3091
8	G	90	4	30	11.7412	-21.3942
9	C	20	4	90	6.2525	-15.9210
10	C	40	5	60	11.2415	-21.0164
11	C	60	2	30	8.6451	-18.7354
12	C	90	3	15	9.3254	-19.3933
13	H	20	5	30	4.7541	-13.5413
14	H	40	4	15	5.5462	-14.8799
15	H	60	3	90	8.5402	-18.6293
16	H	90	2	60	9.5408	-19.5916

The examination delineated the hierarchy of control parameters as impact velocity (B), Coating material (A), Impingement angle (D), and discharge rate (C) in descending order of significance. Consequently, impact velocity emerged as the predominant factor influencing erosion wear rate, with discharge rate exhibiting relatively lower significance.

Moreover, the maximum delta value signifies the most influential parameter on erosion wear rate.

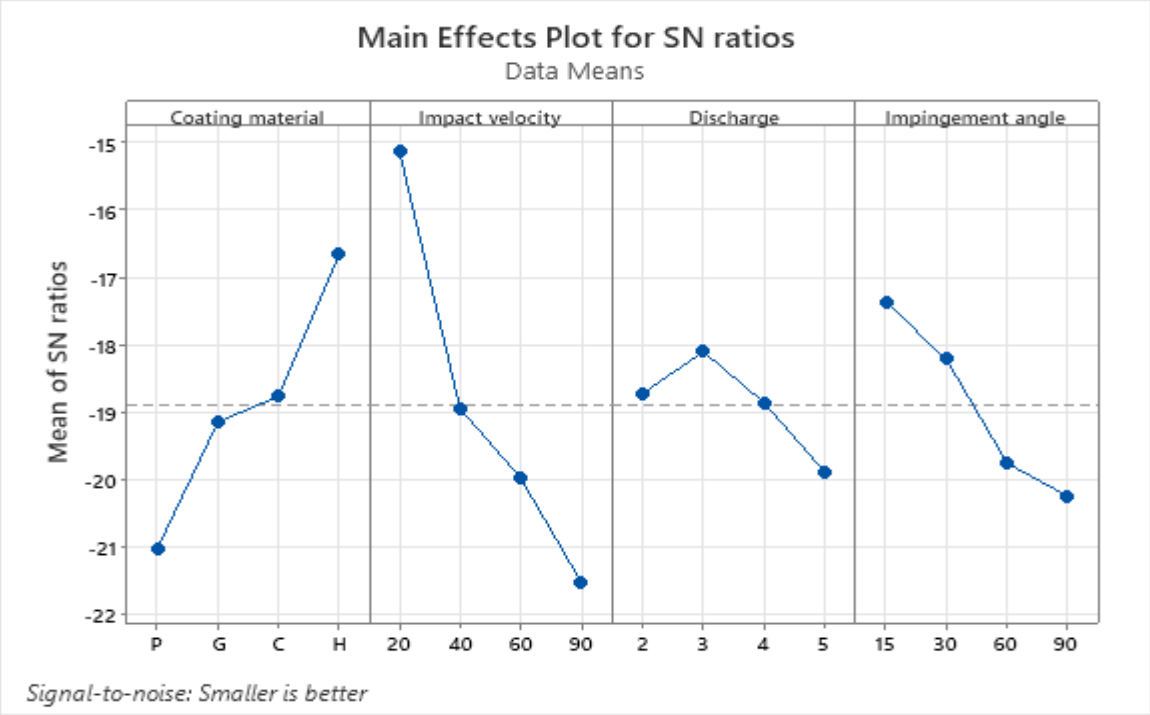

Figure 6.3 Impact of influencing variables on erosion wear rate (Mean of S/N ratios).

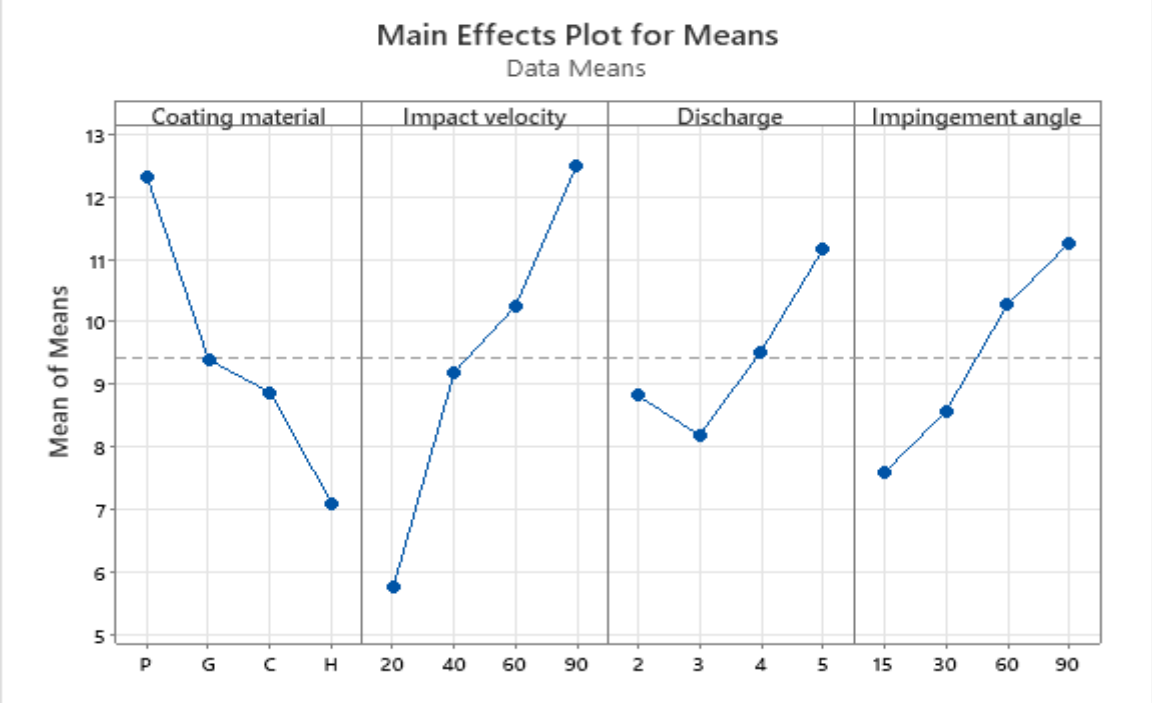

Figure 6.4 Impact of influencing variables on erosion wear rate (Mean of Means).

Table 6.4 Signal-to-noise (S/N) ratio response table for minimum erosion rate (From Taguchi analysis)

Level	Coating material	Impact velocity	Discharge rate	Impingement angle
1	-21.03	-15.14	-18.74	-17.37
2	-19.15	-18.95	-18.1	-18.22
3	-18.77	-19.98	-18.86	-19.76
4	-16.66	-21.53	-19.9	-20.25
Delta	4.37	6.39	1.8	2.87
Rank	2	1	4	3

Table 6.5 The Mean of the means response table for minimum erosion rate (from the Taguchi analysis)

Level	Coating material	Impact velocity	Discharge rate	Impingement angle
1	12.318	5.749	8.82	7.588
2	9.392	9.19	8.184	8.566
3	8.866	10.242	9.522	10.269
4	7.095	12.491	11.146	11.249
Delta	5.223	6.741	2.963	3.661
Rank	2	1	4	3

6.3 Analysis of variance (ANOVA) and the effects of factors

ANOVA (Analysis of Variance) was employed to discern the primary design parameters significantly influencing the quality attribute in the study. Factors under investigation included coating material (A), impact velocity (B), discharge rate (C), and impingement angle (D), analyzed using MINITAB 18. Table 6.6 summarizes the ANOVA findings for the signal-to-noise ratio, with a confidence level of significance set at 95%.

The F-value, computed for each design parameter, indicated significance, with factors surpassing an F-value of four deemed notably influential in shaping the optimal characteristic. The analysis revealed that impact velocity (B), coating material (A), and impingement angle (D) emerged as notably significant factors, whereas discharge rate (C) displayed relatively less significance. The significance of the P-value, evaluated alongside, underscored the importance of factors with a P-value less than 0.05 ($P < 0.05$) [186]. Additionally, the final column of Table 6.6 illustrates the percentage contribution of each parameter to the total variation, elucidating their individual impacts on the outcome. ANOVA results confirmed that impact velocity was the most dominant factor influencing erosion wear, contributing 56.53%, followed by coating material (24.47%) and impingement angle (14.77%), while discharge rate had the least effect (4.23%) [251]. These findings align with previous studies [252, 253], emphasizing impact velocity as a critical determinant of erosion wear in polymer composites. Higher velocities increase kinetic energy transfer, leading to more significant material loss, while optimized nanocoatings enhance stress dissipation and minimize surface damage.

Table 6.6 ANOVA analysis of polymer composites

Source	DF	Adj SS	Adj MS	F	P	Contribution (%)
Coating material	3	38.469	12.8231	21.62	0.016	24.468
Impact velocity	3	88.883	29.6278	49.94	0.005	56.535
Discharge rate	3	6.658	2.2193	3.74	0.154	4.234
Impingement angle	3	21.426	7.142	12.04	0.035	13.628
Residual Error	3	1.78	0.5932			1.132
Total	15	157.216				

The significant influence of coating material further supports prior research, demonstrating that functionalized nanoparticles improve interfacial adhesion, inhibit crack propagation,

and enhance energy absorption during impact. These insights highlight the crucial role of impact velocity, coating material, and impingement angle in optimizing the erosion resistance of polymer composites, offering valuable guidelines for improving their durability in high-wear applications.

6.4 Impact of CNTs, GO, and hybrid (CNTs/GO) coating on the erosive wear properties of carbon fiber reinforced polymer composites.

Figure 6.5 illustrates the erosion wear rates of polymer composites C1, C2, C3, and C4 under uniform test conditions, including an impact velocity of 60 m/s, discharge rate of 4 g/min, and an impingement angle of 60°, facilitating direct comparison among the composites. Notably, C2, C3, and C4 composites exhibit reduced erosion wear rates compared to C1, attributed to the incorporation of CNTs, GO, or a combination of both as coatings on the carbon fiber within the polymer composite. The enhancement of interfacial adhesion by these coatings contributed to the improved resistance to wear. Specifically, the erosion wear rate of C1 composite is measured at 14.576($x10^{-5}$ g/g). Comparative analysis reveals a 28.76% decrease in erosive wear rate for C2 compared to C1, attributed to the improved interfacial adhesion induced by the wrinkled, rough surface of GO [239, 240]. Similarly, C3 demonstrates a significant 32.24% decrease in erosive wear rate compared to C1, owing to the reinforcing effect of CNTs on the matrix, which improves erosion wear resistance by distributing stress and absorbing impact energy [254]. Furthermore, C4 exhibits the lowest erosion wear rate, 44.56% less than C1, attributed to the synergistic effect of CNTs/GO hybrid coating on carbon fiber reinforced polymer composite. These results correlate with previous studies [255-257], that emphasize the role of nanoparticles in reinforcing fiber-matrix interfaces, thereby improving mechanical stability and reducing material degradation under erosive conditions. The hybrid coating promotes the formation of a 3D structure of hybrid carbon nanomaterials, increasing surface area and enhancing

contact and interlocking at the interface between the matrix and carbon fibers. Additionally, the uniform dispersion of stress throughout the matrix further enhances wear resistance [242]. The findings showed great enhancement in erosion wear properties due to the surface modification of carbon fiber with CNTs and GO.

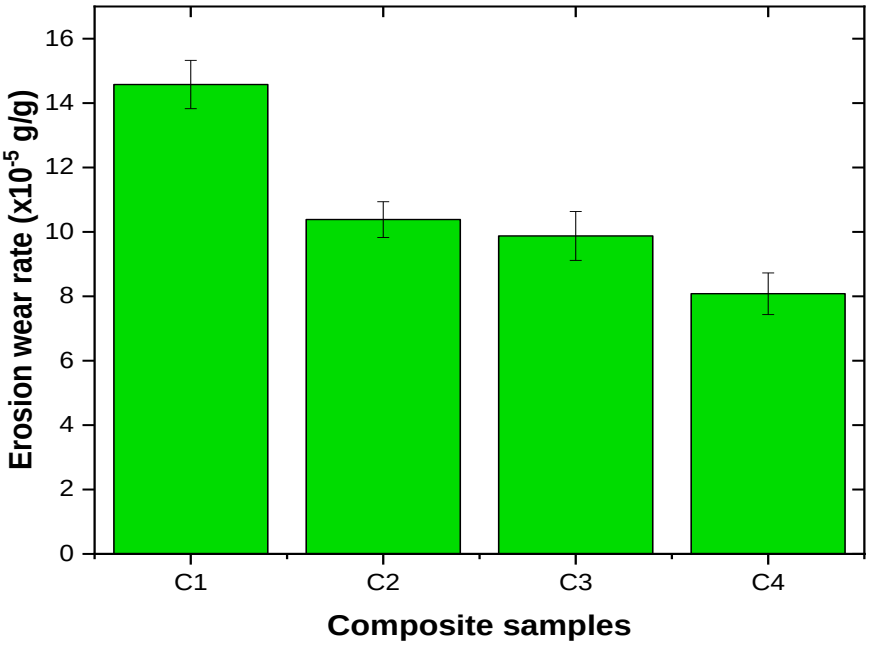

Figure 6.5 Erosion wear rate of C1, C2, C3, and C4 polymer composites at impact velocity of 60 m/s, discharge rate of 4 g/min, and an impingement angle of 60°.

6.5 SEM analysis of worn surfaces

SEM images of the degraded surfaces of composite specimens were employed to identify the main factors which impacting on the erosion wear. The interactions between the polymer matrix and CNT/GO-coated fibers in reinforced polymer composites are governed by interfacial adhesion, mechanical interlocking, and load transfer efficiency. The oxygen-containing functional groups in GO enhance chemical bonding with the epoxy matrix, improving fiber wettability and adhesion, while CNTs strengthen fiber-matrix interactions through π–π interactions and high surface area contact [258]. The irregular surface texture of GO promotes mechanical interlocking, preventing fiber pull-out, while CNTs create a

nanoscale interphase layer that resists shear forces and bridges microcracks [259, 260]. This synergistic effect improves stress distribution, where CNTs act as load carriers, transferring stress efficiently from the matrix to the fibers, and GO dissipates impact energy, reducing stress concentration. Under erosive conditions, CNT/GO-coated fibers minimize surface degradation by restricting material removal, reducing fiber exposure, and enhancing matrix erosion resistance.

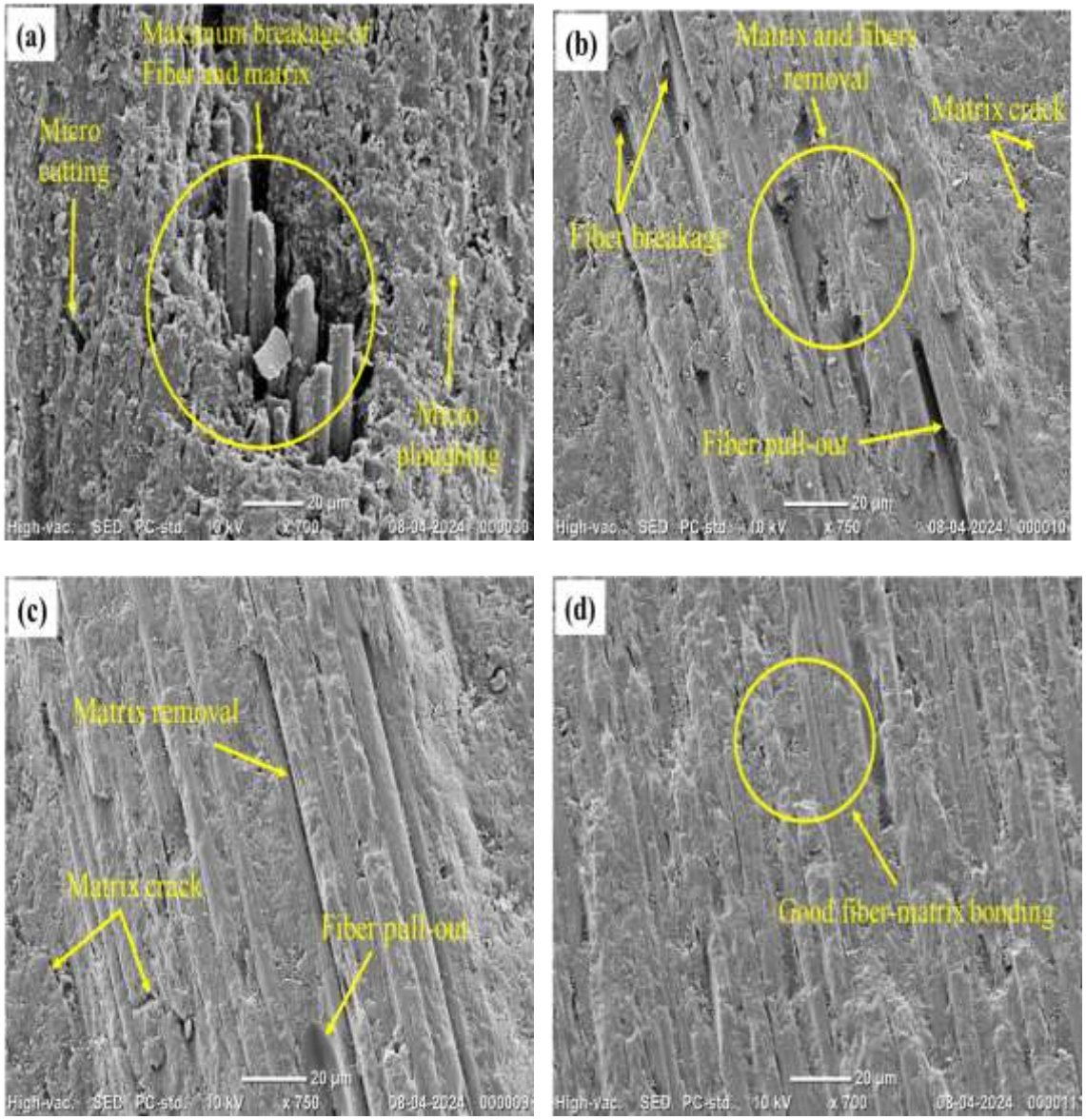

Figure 6.6 SEM image of erodent surface of (a) C1, (b) C2, (c) C3, and (d) C4 polymer composites under the same condition, the impact velocity of 60 m/s, discharge rate of 4 g/min, and an impingement angle of 60°.

As depicted in Figure 6.6(a), it is apparent that micro-cutting and indications of micro-plowing phenomena are predominantly observed in the polymer composites. These phenomena led to extensive matrix and fiber breakage in the C1 composite, contributing to significant erosion wear [261]. At elevated loads, the sharp edges of abrasive particles induce the initiation of cracks within the matrix, leading to the formation of high-stress concentrations. Subsequently, these cracks propagate, causing matrix damage, which exposes the fibers to the abrading environment, leading to fiber breakage [262]. The incorporation of GO/CNTs facilitated the ability of fibers to withstand high abrading loads by diffusing between the fabric layers and fibers, thereby enhancing the erosion wear resistance of the composite [263, 264]. Furthermore, the presence of GO/CNTs or both in the composites enhanced the adhesion and mechanical interlocking between the matrix-fiber interfaces, thereby augmenting wear resistance. Figures 6.6(b), (c), and (d) illustrated reduced matrix damage and favourable fiber-matrix adhesion, crucial factors contributing to wear reduction. Among the four composites, C4 exhibited minimal fiber and matrix breakage due to its strong fiber-matrix bonding, as depicted in Figure 6.6(d), resulting in improved erosion resistance strength of the composite.

Figure 6.7(a) illustrates the presence of both the damaged matrix and the emergence of ripple patterns on the composite surface. These ripple patterns are to be expected, since particles with small impact angles generate abrasion rather than erosion, as they are practically flush or grazing manner with the surface of polymer rather than directly perpendicular [255]. This grazing impact angle leads to erosion of the surface material in a way that produces wave-like patterns or ripples. These patterns manifest as irregularities or undulations on the surface of the composite material. The emergence of ripple patterns signifies the directional nature of erosion wear and offers insights into the erosive mechanisms affecting the composite surface. Understanding the formation and

characteristics of these ripple patterns can be instrumental in evaluating the erosion resistance of the composite material and optimizing its performance in erosive environments.

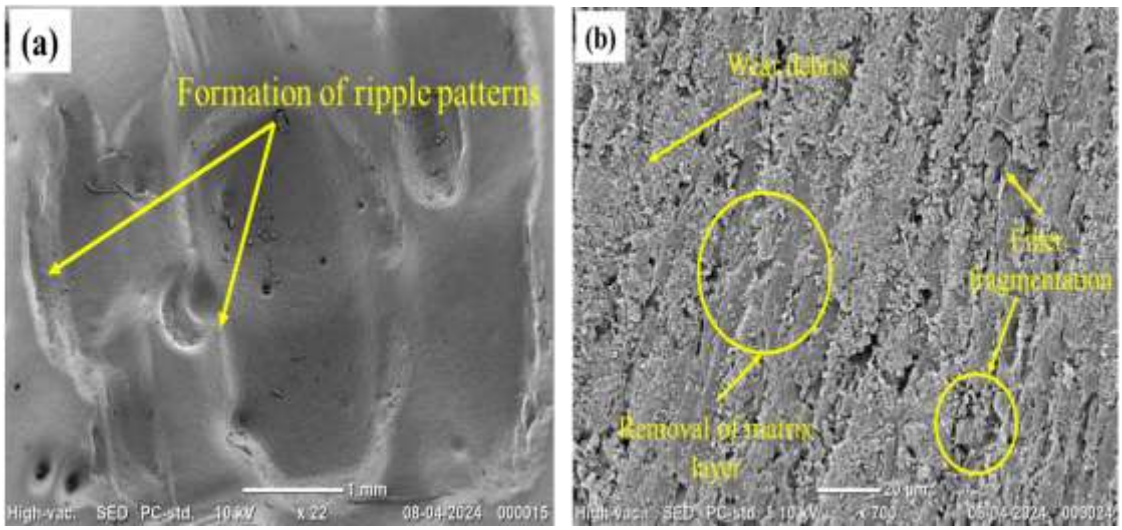

Figure 6.7 SEM image of C4 under conditions (a) impact velocity of 40 m/s, discharge rate of 4 g/min, and an impingement angle of 15°, (b) impact velocity of 60 m/s, discharge rate of 3 g/min, and an impingement angle of 90°.

In Figure 6.7(b), several important observations can be made. Firstly, broken carbon fibers are clearly visible, exposing the internal structure of the composite material. Additionally, wear debris can be seen scattered across the surface, indicating the effects of erosion wear. Furthermore, the fibers are exposed due to the removal of matrix layers. It is apparent that cracks have originated from the impact point and have subsequently extended, leading to the breaking of the fibers into smaller fragments. The presence of multiple intersecting cracks suggests a complex fracture pattern, likely induced by the impact forces. Moreover, the formation of wear debris can be attributed to brittle fracture in the fiber body. With repetitive impacts, this debris accumulates on the surface and contributes to the measured wear loss [251]. The presence of furrows as shown in Figure 6.8(a) exclusively at the entry surface in the erosion test suggests localized and concentrated erosion effects at the point where the erodent first impacts the material. This phenomenon is often observed due to the

initial high-velocity impact of the erodent particles, which leads to significant material removal and the formation of pronounced surface features such as furrows or grooves.

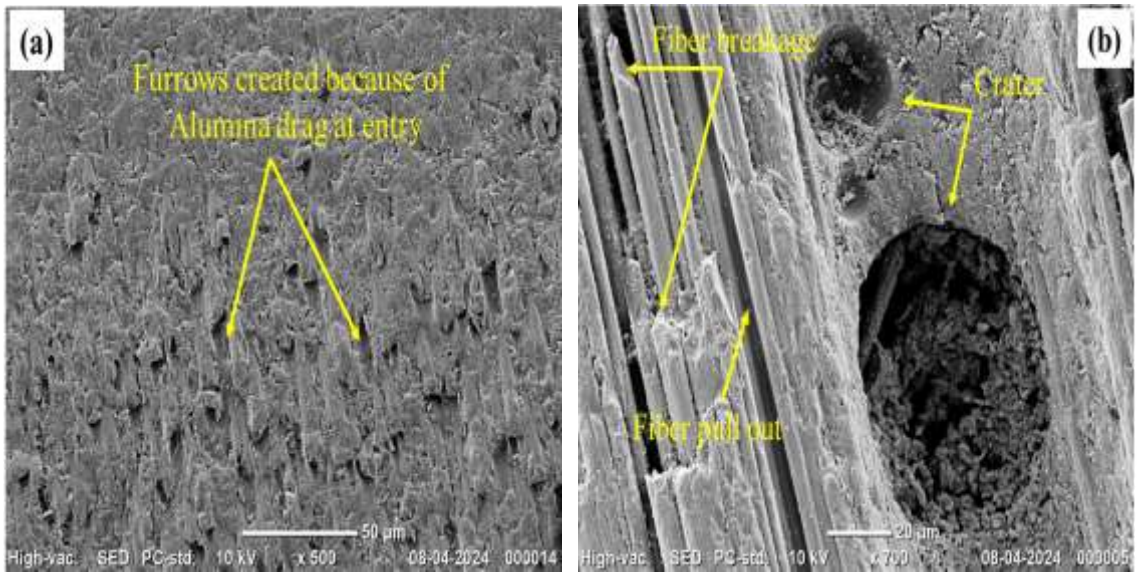

Figure 6.8 SEM image of C1 under conditions (a) impact velocity of 30 m/s, discharge rate of 3 g/min, and an impingement angle of 30°, (b) impact velocity of 90 m/s, discharge rate of 5 g/min, and an impingement angle of 90°.

These deep furrows indicate the severity of erosion wear at the entry point, highlighting the area most susceptible to erosive damage [262]. Figure 6.8(b) depicts the eroded surface's microstructure, revealing the craters' presence. These craters are formed as a result of material removal due to erosion wear. During the erosion process, high-velocity particles, with high impingement angles, or abrasive agents impact the surface, causing localized damage and material displacement. The repeated impingement of these particles leads to the formation of depressions or craters on the surface, as observed in the microstructure [265]. The failure mechanism in CF/epoxy composite is a multifaceted process characterized by the removal of surface matrix, the development of surface micro-cracks, debonding between fiber and matrix, fracture of fibers, and material removal [266-268].

6.6 Summary

From the above results and discussion, the findings can be summarized as follows:

- This study analyzed the erosion wear performance of epoxy composites in which erosion resistance was primarily governed by impact velocity, with a lesser influence from discharge rate.
- The hybrid CNT/GO-coated composite (HCFRE) exhibited the highest erosion resistance, reducing the wear rate by 44.56% compared to uncoated CFRE.
- The enhancements were attributed to the synergistic effect of CNTs and GO, forming an interconnected network that improved stress distribution, crack resistance, and fiber-matrix adhesion.
- SEM analysis identified the key erosion wear mechanisms, including micro-cutting, plowing, matrix-fiber debonding, and material loss.
- The study highlights the potential of CNT/GO hybrid coatings for aerospace and structural applications.